23rd IEEE International Symposium on Personal, Indoor and Mobile Radio Communications (PIMRC 2012)

Self-Organizing Ad Hoc Femtocells for Cell Outage Compensation Using Random Frequency Hopping

Markus Putzke and Christian Wietfeld

Communication Networks Institute (CNI)
TU Dortmund University, 44227 Dortmund, Germany
{Markus.Putzke, Christian.Wietfeld}@tu-dortmund.de

***Abstract*—This paper analyzes self-organization of ad hoc femtocells within a macrocell infrastructure by using random frequency hopping. Femtocell users select their frequency subbands randomly, so that corresponding femtocells are capable of integrating themselves into macrocells without any exchange of information. No sensing equipment is required in femtocell devices and no time is consumed for self-organization. This makes random frequency hopping highly attractive as a self-organization policy in outage situations, i.e. where macrocell base stations fail and immediate coverage has to be provided by femtocells. We present an exact analytical model for the Bit Error Rate (BER) of femtocell users and access points using random frequency hopping, based on Signal to Interference and Noise Ratio (SINR) and Laplace transform techniques. Moreover, for performance evaluation, the model is applied to frequency-nonselective and frequency-selective channels and is verified by simulations implemented in MATLAB. The results of random frequency hopping are compared to classical resource planning with orthogonal patterns and to systems without resource planning. It is shown that random frequency hopping introduces a reduction of the BER up to a factor of 7 compared to systems where the interferer is transmitting in the same subband as the femtocell user.**

I. Introduction

Femtocells are constantly gaining attraction, as they offer extended coverage and broadband services. They are based on Orthogonal Frequency Division Multiple Access (OFDMA) systems which increase the spectral efficiency and throughput, while simultaneously decreasing power consumption compared to other multiple access technologies.

As mobile traffic is increasing approximately 30% each year [1], the cell coverage is constantly decreasing. Hence, the provision of broadband services requires small cells with a great spatial reuse of the radio resources. Femtocells counter this problem of enhanced system capacities, however they introduce severe interference problems with existing macrocells, as they are using the same radio resources.

Since femtocells are typically used to extend indoor coverage or to offload traffic from macrocells, common applications result in an overlay with existing Long Term Evolution (LTE) macrocells. Due to the fact that centralized orthogonal resource planning, which is classically done in macrocells, would require a high administrative overhead in femtocells, both cells normally share the same resources which introduces interference. In the following, we concentrate on the interference between femto- and macrocells which represents the major problem when femtocells are well separated. Fig. 1 depicts the situation in the downlink, where the macrocell base station interferes with a femtocell user. In contrast, Fig. 2 shows the uplink, where a macrocell user interferes with the femtocell access point. If femtocell users are allowed to allocate frequency subbands simultaneously, interference among them also occurs. Although the uplink in LTE is realized as Single Carrier Frequency Division Multiple Access (SC-FDMA), it can be interpreted as linearly precoded OFDMA with the same Symbol Error Rate (SER) as classical OFDMA.

Due to these problems, self-organization techniques are required, which allow femtocells to integrate themselves with a minimal amount of interference. Different self-organization methods are known which can be categorized into centralized and distributed ones. Centralized approaches are realized e.g. by fractional frequency reuse, where subbands for cell edge users are orthogonally selected in relation to users of adjacent cells [2]. Distributed self-organization is commonly based on sensing the environment, such as exploring the used resources of the surrounding cells. Famous distributed methods are time and frequency Inter-Cell Interference Coordination (ICIC) [3]. Time ICIC is based on protected and non-protected resources, which indeed reduces interference but also throughput. In contrast, frequency ICIC is realized by sensing the control channel of the macrocell and adjusting the femtocell resources [4]. Another way to reduce interference is power control. A good overview of self-organization techniques is given in [5].

In this paper, we propose to use dynamical hopping patterns in the femtocell which are randomly chosen by the users. Thereby, the femtocell is able to integrate itself into the macrocell with limited interference, but without any exchange of information, centralized planning and sensing. In other words, the inter-cell interference is reduced by scrambling it within the used channel bandwidth. Each transmitter chooses a random hopping pattern before transmission according to a given probability density function (pdf) and informs the receiver about the selected pattern. As a consequence, no cell-discovery of the environment is required, so that femtocells can immediately operate without delay after activation. Thus Random Frequency Hopping OFDMA (RFH-OFDMA) systems are highly attractive in outage situations when macrocell

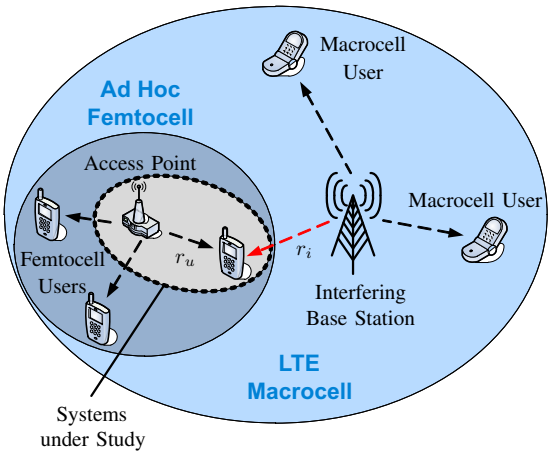

Fig. 1. Inter-cell interference in the downlink (OFDMA)

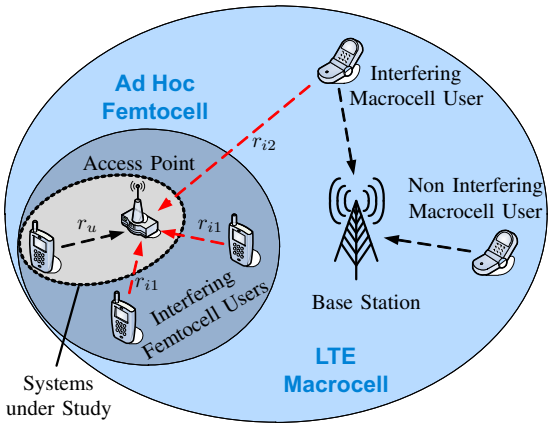

Fig. 2. Inter-cell interference in the uplink (SC-FDMA)

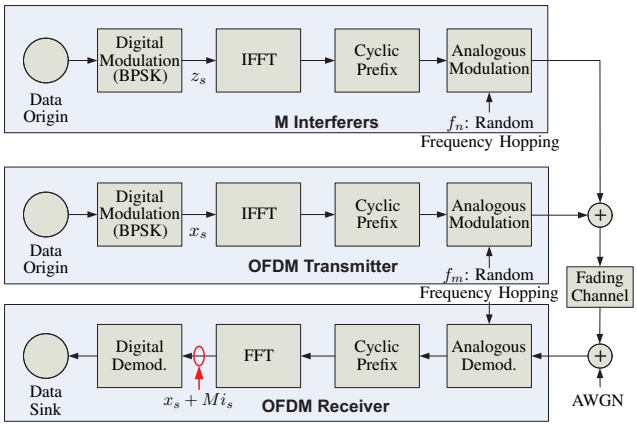

Fig. 3. Block diagram for analytical model and simulations

base stations fail and capacity has to be provided immediately by femtocells. For those situations, it is beneficial to have a wireless femtocell backhaul, e.g. by using Unmanned Aerial Vehicles as flying femtocell access points [6]. Another advantage of RFH-OFDMA is an increase in user capacity and spectral efficiency, as these systems allow to occupy subcarriers by more than one user for a short time. The application of random frequency hopping within OFDMA systems were first introduced in [7]. Two fundamental situations will be discussed throughout the paper: in scenario one, all random frequency hopping patterns are independent, which results in inter- as well as intra-cell interference, cf. Figures 1 and 2. In contrast, scenario two uses a coordinated orthogonal but random approach within the femtocell such that only inter-cell interference occurs.

Due to the fact that orthogonal hopping patterns of macrocells are also random from the perspective of femtocell users in our approach, we consider interfering RFH-OFDMA systems in the following. The key challenge is to quantify how much interference is introduced by the random hopping patterns. Existing approaches like [8] and [9] determine the system performance only by simulations and/or without considering the signal processing in the transmitter and receiver. In order to capture the performance of self-organizing RFH-OFDMA systems, we present an analytical model deriving the BER and verify it with simulations implemented in MATLAB. Furthermore, the analytical model is applied to Rayleigh and Rice fading in frequency-nonselective and frequency-selective channels. In contrast to simulations, as shown in [10], the analytical BER model provides insight into system design guidelines and key performance indicators. It allows to analyze influences of time and frequency parameters like the user bandwidth, the number of subcarriers and the guard time as well as channel parameters like the Ricean K-factor or number of received multipaths. Regarding these parameters, we focus on typical values of LTE in our analysis. Moreover, the impact of different pdfs for the random hopping patterns is examined, which has also not been considered by previous works. In order to quantify the achieved improvements, we compare the results with the performance of systems using an ideal centralized and orthogonal resource planning and of systems using neither orthogonality nor resource planning.

The analysis starts with a system model in section II. In section III, the analytical model for the BER is derived as a function of different fading channels. Section IV then illustrates the results derived from the analytical and simulation model, followed by the conclusion in section V.

II. System Model

In this section, the overall structure of the analytical and simulation model is shown. Fig. 3 depicts a block diagram of the components needed to model the interference situations of Figures 1 and 2 when M interferers are supposed. Each interfering system consists of a basic digital modulator, which is assumed to use Binary Phase Shift Keying (BPSK), an inverse Fourier transformation ensuring the orthogonality of OFDMA, an addition of a cyclic prefix and an analogous modulation using random carrier frequencies over time. The OFDM transmitter and receiver of the interfered system comprises the same components, with the only difference that an identical random carrier frequency pattern is used. Furthermore, the symbols of the interferers are denoted by z_s and those of the OFDM transmitter by x_s. Thus, the detected symbols in the interfered system are composed of x_s and the symbols of the interfering systems i_s.

In [10] we have shown that the interference signal of one user in such an environment can be described at the output of the decision device in the receiver by

$$i_s = A \sum_{l=-\infty}^{\infty} \sum_{d=0}^{N_n-1} \frac{z_{d,l} \mathrm{Re}\left\{\beta_{s,d,l}\right\}}{\sqrt{D_n D_m}} , \tag{1}$$

where

$$\beta_{s,d,l} = \frac{e^{\mathrm{j}2\pi[Q_m s C_m - Q_n d(lT_n + C_n)]}}{\mathrm{j}2\pi\left[Q_n d - Q_m s + f_x\right]} \times \left(e^{\mathrm{j}2\pi U[Q_n d - Q_m s + f_x]} - e^{\mathrm{j}2\pi L[Q_n d - Q_m s + f_x]}\right) \tag{2}$$

and

$$\begin{aligned} L &= \max\left\{C_m, lT_n\right\} \\ U &= \min\left\{T_m, (l+1)T_n\right\} . \end{aligned} \tag{3}$$

Here N represents the number of subcarriers, T the symbol duration, C the guard interval, D the data carrying part, Q the subcarrier spacing, d the subcarrier index, l the symbol index and $z_{d,l}$ the transmitted symbols of the interferer. Moreover, subscript n is used for parameters of the interfering and m for parameters of the interfered system. The random frequency hopping is included in the term f_x, which characterizes the difference between the carrier frequencies of the interfering and interfered system $f_n - f_m$, cf. Fig. 4. Since f_n and f_m are varying according to a specific pdf, f_x is also randomly changing with time.

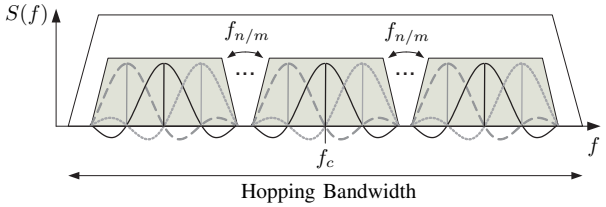

Fig. 4. Realization of frequency hopping

III. Analytical Model for the BER

In this section, an exact analytical model for the BER of femtocells using random frequency hopping within a macrocell infrastructure is derived and applied to different fading channels, such as Rayleigh and Rice in frequency-nonselective and frequency-selective environments. We begin by deriving a model for the BER conditioned on fixed large-scale fading, i.e. random small-scale variations are omitted first. Afterwards the model will be extended by random fluctuations of the fading amplitude.

A. Analytical Model for Fixed Fading Amplitudes

The BER caused by M interfering RFH-OFDMA systems can be determined based on (1). If a BPSK with equal symbol probability is assumed, the BER equals the SER and is independent of the transmitted symbols

$$\mathrm{BER}_s = \int_{-\infty}^{-g_s} p_{r_s}(x)\mathrm{d}x \,. \tag{4}$$

Here p_{r_s} denotes the pdf of the sum of interference symbols in the receiver

$$r_s = \sum_{m=1}^{M} i_s + n_s \,, \tag{5}$$

while n_s represents Additive White Gaussian Noise (AWGN) and g_s the frequency domain channel gain. Equation (4) depends on the subcarrier s and therefore has to be averaged in order to get the overall BER. Since it is very difficult to determine the pdf of r_s, we rearrange (4) with the help of Laplace transform techniques

$$\mathrm{BER}_s = \frac{1}{2\pi\mathrm{j}} \int_{c-\mathrm{j}\infty}^{c+\mathrm{j}\infty} \int_{-\infty}^{-g_s} \mathrm{e}^{\gamma x} \mathcal{L}\left\{p_{r_s}\right\}(\gamma)\mathrm{d}\gamma\mathrm{d}x \tag{6}$$

where $\mathcal{L}\{\cdot\}(\gamma)$ denotes the Laplace transform to variable γ. After some straightforward analysis, this can be written as

$$\mathrm{BER}_s = \frac{1}{2\pi\mathrm{j}} \int_{c-\mathrm{j}\infty}^{c+\mathrm{j}\infty} \mathbb{E}\left\{\mathrm{e}^{-\gamma r_s}\right\} \frac{\mathrm{e}^{-\gamma g_s}}{\gamma}\mathrm{d}\gamma \,. \tag{7}$$

Compared to (4) the advantage is that all parameters can be evaluated numerically. Beginning with the expectation of the interference symbols, we get

$$\mathbb{E}\left\{\mathrm{e}^{-\gamma r_s}\right\} = \int_{-\infty}^{\infty} \mathrm{e}^{-\gamma r_x} p_{r_s}(x)\mathrm{d}x \,. \tag{8}$$

As the symbols of the interferers i_s are independent among each other as well as independent of the AWGN signal n_s, the pdf p_{r_s} can be factorized

$$p_{r_s} = p_{i_s}(x_1)p_{i_s}(x_2)\cdots p_{i_s}(x_M)p_{n_s}(x_{M+1}) \,, \tag{9}$$

which results in

$$\mathbb{E}\left\{\mathrm{e}^{-\gamma r_s}\right\} = \left[\mathbb{E}\left\{\mathrm{e}^{-\gamma i_s}\right\}\right]^M \mathbb{E}\left\{\mathrm{e}^{-\gamma n_s}\right\} \,. \tag{10}$$

The Laplace transform of the AWGN can be easily calculated

$$\mathbb{E}\left\{\mathrm{e}^{-\gamma n_s}\right\} = \exp\left(\frac{\sigma_n^2\gamma^2}{2}\right) \,, \tag{11}$$

where σ_n is the average power of the AWGN. It remains to determine the Laplace transform of the interference i_s. If we make use of (1) and the fact that the transmitted symbols $z_{d,l}$ are stochastically independent of the symbol index l as well as of the subcarrier index d, we get

$$\mathbb{E}\left\{\mathrm{e}^{-\gamma i_s}\right\} = \mathbb{E}\left\{\prod_{l=-\infty}^{\infty}\prod_{d=0}^{N_n-1} \exp\left(-\gamma A\frac{z_{d,l}\mathrm{Re}\left\{\beta_{s,d,l}\right\}}{\sqrt{D_n D_m}}\right)\right\} \,. \tag{12}$$

Note that (12) comprises two random variables, $z_{d,l}$ and f_x, since the fading amplitude A is still fixed at this point. As the transmitted symbols and the random carrier frequencies are also stochastically independent, both expectations can be evolved consecutively

$$\mathbb{E}\left\{\mathrm{e}^{-\gamma i_s}\right\} = \mathbb{E}\left\{\mathbb{E}\left\{\mathrm{e}^{-\gamma i_s}\right\}\big|_{f_x}\right\} \tag{13}$$

where $\mathbb{E}\{\cdot\}|_x$ denotes the conditional expectation when x is fixed. For simplicity of notation we denote the conditional expectation in (13) by $\mathbb{E}_{i_s}|_{f_x}$ and the overall expectation by $\mathbb{E}_{i_s}$. Considering that $z_{d,l}$ only takes the values ±1, (13) results as

$$\mathbb{E}_{i_s} = \mathbb{E}\left\{\prod_{l=-\infty}^{\infty}\prod_{d=0}^{N_n-1} \cosh\left(\frac{\gamma A}{\sqrt{D_n D_m}}\mathrm{Re}\left\{\beta_{s,d,l}\right\}\right)\right\} \,. \tag{14}$$

We are left with the expectation dependent on the random carrier frequencies f_x. Given an arbitrary pdf $p_{f_x}(x)$ for the random carrier frequencies, cf. Fig. 4, the overall Laplace transform of the interference yields

$$\mathbb{E}_{i_s} = \int_{-\infty}^{\infty} \mathbb{E}_{i_s}|_{f_x}\, p_{f_x}(x)\mathrm{d}x \,, \tag{15}$$

which can be solved using numerical evaluation. All we need to do is to insert (10), (11) and (15) into the equation for the BER (7). Since the complex contour integral in (7) does not have a closed form solution, we resort to the effective Gauss-Chebyshev approximation, cf. [11]. In this manner, the BER can be expressed as

$$\begin{aligned}\mathrm{BER}_s \approx &\frac{1}{\nu}\sum_{k=1}^{\nu/2} \mathrm{Re}\left\{\mathrm{e}^{\frac{\sigma_n^2 c^2\lambda_k^2}{2}}\left[\mathbb{E}\left\{\mathrm{e}^{-c\lambda_k i_s}\right\}\right]^M \mathrm{e}^{-c\lambda_k g_s}\right\} + \ldots \\ &\tau_k \mathrm{Im}\left\{\mathrm{e}^{\frac{\sigma_n^2 c^2\lambda_k^2}{2}}\left[\mathbb{E}\left\{\mathrm{e}^{-c\lambda_k i_s}\right\}\right]^M \mathrm{e}^{-c\lambda_k g_s}\right\} \,,\end{aligned} \tag{16}$$

where

$$\lambda_k = 1 + \mathrm{j}\tau_k \quad \text{and} \quad \tau_k = \tan\left(\frac{(2k-1)\pi}{2\nu}\right) . \tag{17}$$

The parameter c is chosen such that the integrand in (7) multiplied by γ is minimum, which corresponds to the Chernoff-bound

$$\min_c \left\{ \exp\left(\frac{\sigma_n^2 c^2}{2}\right) \mathbb{E}\left\{\mathrm{e}^{-ci_s}\right\} \mathrm{e}^{-cg_s} \right\} . \tag{18}$$

Since (16) represents the BER per subcarrier s, the overall BER is achieved by averaging (16) over N_n. Note that (16) not only holds for the OFDMA downlink, it holds for the SC-FDMA uplink as well if we replace the BER by the SER.

B. Analytical Model for the BER in Frequency-Nonselective Channels

After having derived a model for the BER conditioned on fixed fading, we will now drop this assumption and extend the model for different types of small scale fading. At first we determine an expression for frequency-nonselective fading. In this case (16) has to be averaged over the pdfs of the fading amplitudes A and g_s

$$\mathrm{BER}_s = \frac{1}{2\pi\mathrm{j}} \int_{c-\mathrm{j}\infty}^{c+\mathrm{j}\infty} \mathbb{E}_{n_s} \left[\int_0^\infty \mathbb{E}_{i_s} p_r(x) \mathrm{d}x \right]^M \frac{\mathbb{E}\left\{\mathrm{e}^{-\gamma g_s}\right\}}{\gamma} \mathrm{d}\gamma . \tag{19}$$

Here $p_r(x)$ denotes the pdf of the fading amplitude A and $\mathbb{E}_{n_s}$ is an abbreviation for (11). In the case of Rayleigh fading, the expectation of the frequency domain channel gain g_s results in the closed form solution

$$\mathbb{E}\left\{\mathrm{e}^{-\gamma g_s}\right\} = 1 - \sqrt{2\pi}\sigma\gamma \mathrm{e}^{\frac{\sigma^2\gamma^2}{2}} Q\left(\sigma\gamma\right) . \tag{20}$$

In contrast, for frequency-nonselective Rice fading, the expectation of g_s has to be numerically solved

$$\mathbb{E}\left\{\mathrm{e}^{-\gamma g_s}\right\} = \int_0^\infty \mathrm{e}^{-\gamma x} \frac{x}{\sigma^2} \exp\left(-\frac{x^2+v^2}{2\sigma^2}\right) I_0\left(\frac{xv}{\sigma^2}\right) \mathrm{d}x , \tag{21}$$

where v represents the noncentrality parameter and I_0 the zero-order modified Bessel function of the first kind.

C. Analytical Model for the BER in Frequency-Selective Channels

Next we extend our analytical approach for frequency-selective channels. As frequency-selective transmissions suffer from multipath propagation, the superposition of different interference signals i_s as well as signals from the OFDM transmitter g_s, each having a own fading amplitude and phase shift, have to be considered. In order to facilitate the model we assume a RAKE receiver, which is able to cancel out the different phase shifts of the individual signals, i.e. all signals are added coherently in the receiver. Under this assumption the BER gets

$$\mathrm{BER}_s \approx \frac{1}{2\pi\mathrm{j}} \int_{c-\mathrm{j}\infty}^{c-\mathrm{j}\infty} \mathbb{E}\left\{ \mathrm{e}^{-\gamma \sum_{l=1}^{L} r_s} \right\} \frac{\mathbb{E}\left\{ \mathrm{e}^{-\gamma \sum_{l=1}^{L} g_s} \right\}}{\gamma} \mathrm{d}\gamma , \tag{22}$$

where L denotes the number of considered propagation paths. Equation (22) is an approximation, since we assumed that the random carrier frequencies are stochastically independent for different propagation paths. Otherwise it is not possible to derive a closed form expression for the BER. We will find in section IV that the error introduced by (22) is rather small if $L < 4$. As the fading amplitudes of different propagation paths are independent, (22) further simplifies to

$$\mathrm{BER}_s \approx \frac{1}{2\pi\mathrm{j}} \int_{c-\mathrm{j}\infty}^{c+\mathrm{j}\infty} \mathbb{E}_{n_s}^L \left[\int_0^\infty \mathbb{E}_{i_s} p_r(x) \mathrm{d}x \right]^M \frac{\mathbb{E}^L\left\{\mathrm{e}^{-\gamma g_s}\right\}}{\gamma} \mathrm{d}\gamma , \tag{23}$$

where the expectation involving $\mathbb{E}_{i_s}$ has to be performed over the sum of L independent fading amplitudes. In the case of frequency-selective Rayleigh fading, the corresponding distribution can be approximated by [12]

$$p_r(x) \approx \frac{t^{2L-1} \exp\left(-\frac{t^2}{2a}\right)}{2^{L-1} a^L \left(L-1\right)!} , \tag{24}$$

where $t = x/\sqrt{L}$ is the normalized argument and a represents

$$a = \frac{\sigma^2}{L} \left[(2L-1)!!\right]^{1/L} . \tag{25}$$

The double factorial sign corresponds to the definition: $(2L-1)!! = 1 \cdot 3 \cdots (2L-3)(2L-1)$. On the other hand, if we consider frequency-selective Rice fading, the pdf of the sum over L independent fading amplitudes gets [13]

$$p_r(x) \approx \frac{t^L}{c_2^2} \left(\frac{c_1}{c_2 b}\right)^{L-1} \exp\left(-\frac{t^2}{2c_2^2} - \frac{b^2}{2c_1^2}\right) I_{L-1}\left(\frac{tb}{c_1 c_2}\right) , \tag{26}$$

where I_{L-1} is the $L-1$th order modified Bessel function of the first kind, c_1 and c_2 are coefficients taken from [13], t is the normalized argument once again and b is defined as

$$b = \sqrt{\frac{LK\Omega}{K+1}} . \tag{27}$$

Furthermore, K denotes the Rice factor and Ω the normalized average power.

IV. Results and Performance Analysis

In order to evaluate the gain of femtocells using random frequency hopping, a performance analysis is presented in this section. Therefore we analyze two different scenarios: first the femtocell users utilize random patterns in an uncoordinated manner, such that intra- and inter-cell interference occurs, second the femtocell users utilize a random but coordinated approach in a way that intra-cell interference is avoided. For both scenarios the system parameters listed in Table I are used, which are based on the LTE standard [14] and where $P_{TX,f}$ is the transmit power of the femtocell access point. All presented results are based on a worst case analysis, where the femto- as well as the macrocell have maximum load.

We begin by analyzing situation one and assume that the received interference power of the macrocell equals that of the femtocell, i.e. the Signal to Noise Ratio of each interferer is the same. Fig. 5 shows the BER of equation (16) as a function of the interfering distance r_i and of different random hopping distributions, while the distance to the femtocell access point is fixed to r_u=100 m. In order to evaluate the results of random

TABLE I
SYSTEM PARAMETERS

PARAMETER	VALUE
N_n, N_m	120 subcarriers
W_n, W_m	1.8 MHz
C_n, C_m	$0.25N_n/W_n$
T_n, T_m	$1.25N_n/W_n$
Q_n, Q_m	15 KHz
$P_{TX,f}$	23 dBm
SNR	8 dB

frequency hopping, Fig. 5 also shows the BER of systems applying centralized orthogonal planning where no interference occurs and of systems where all interfering systems transmit in the same subband as the interfered system.

Fig. 5 depicts that the BER is decreasing with increasing distance r_i and that Gaussian random frequency hopping always achieves a higher BER as uniform hopping. The reason for this is that uniform hopping, where the carrier frequencies are chosen out of the channel bandwidth with equal probability, uses the whole bandwidth for transmission, while Gaussian hopping prefers the center of the channel for all transmissions. It can be shown that Gaussian hopping always results in less improvements than the uniform one. Therefore, the Gaussian distribution is omitted in all following considerations.

All results in Fig. 5 are verified by simulations implemented in MATLAB (dotted curves). The used simulation model comprises an OFDM transmitter generating random bits according to a BPSK, performing an inverse Fourier transformation, adding a cyclic prefix and transmitting the resulting signal with a random carrier frequency according to the pdf of the frequency hopping, cf. Fig. 3. Afterwards the signal is attenuated according to the fading before the symbols are demodulated in the receiver by another random carrier frequency. The resulting random but uncorrelated BPSK symbols of all interferers are added to the symbols of the interfered system in the receiver.

Fig. 6 shows the dependency of the BER for an increasing channel bandwidth when the distances r_u and r_i are fixed to 100 m. Note that a rising channel bandwidth results in more interferers, since the bandwidth per user is fixed to 1.8 MHz, which increases the BER. Hence the unused bandwidth, which is the difference between the channel bandwidth and occupied bandwidth of all users, varies as a sawtooth function. This free bandwidth cannot be used by cells with centralized planning, but is used by systems with random frequency hopping. Therefore the curves for random frequency hopping show a shape similar to this sawtooth function.

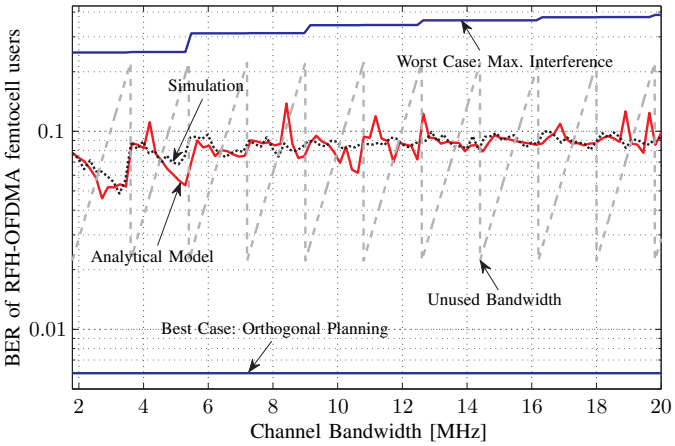

Fig. 6. BER versus channel bandwidth using uniform random frequency hopping and assuming fixed fading amplitudes

The random frequency hopping gain, which is the difference between the BER from section III and the worst case analysis, can be increased in relation to the performance of orthogonal planning, if we assume a coordinated femtocell user approach without intra-cell interference (scenario 2). In the case of frequency-nonselective Rayleigh fading for the femto- as well as for the macrocell, the evaluation of (19) yields the results shown in Fig. 7. As there exists only one interferer in a certain OFDMA timeslot, the interferer of the macrocell, the BER corresponding to the worst case is reduced and represents a horizontal line. Although Rayleigh fading results in simultaneous degradation of received power from the femtocell access point as well as from the macrocell interferer, the random frequency hopping gain increases due to the reduced number of interferers.

In order to increase the random frequency gain further, we analyze the performance within a Rice frequency-nonselective fading, which is shown in Fig. 8. It can be seen that the BER is decreasing as a function of the Rice factor based on an increasing received power at the femtocell users in the downlink and at the femtocell access point in the uplink. It has to be noted that the interference power from the macrocell is simultaneously increasing. The analytical model shows again a good match compared to simulations even if the system contains three random variables: the transmitted symbols, the carrier frequencies and the fading amplitude.

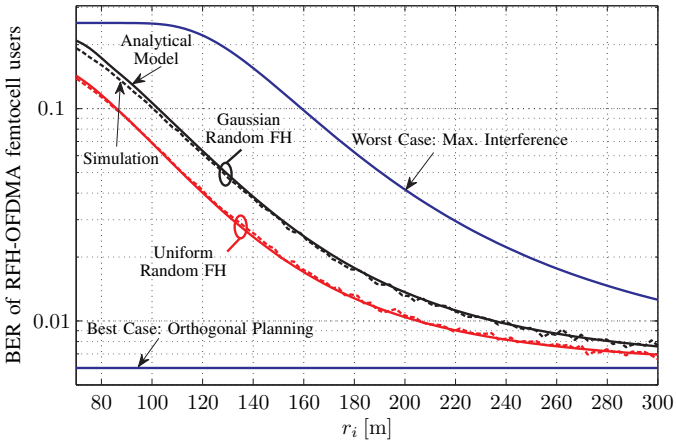

Fig. 5. BER versus distance of the interfering systems r_i with different frequency hopping distributions and a channel bandwidth of 5 MHz

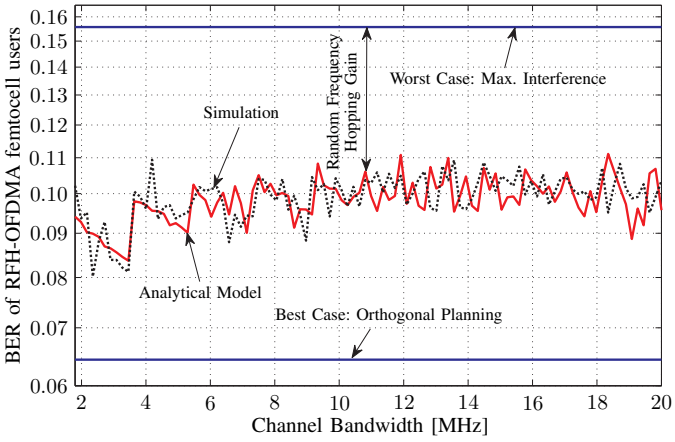

Fig. 7. BER versus channel bandwidth in a Rayleigh frequency-nonselective environment while using uniform random frequency hopping

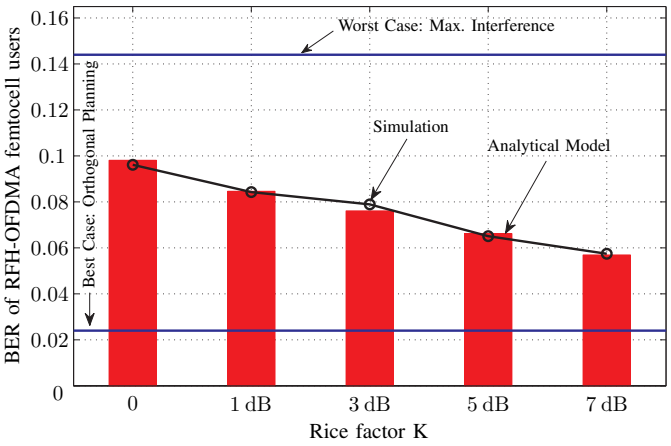

Fig. 8. BER versus Rice factor in a frequency-nonselective channel while using uniform random frequency hopping

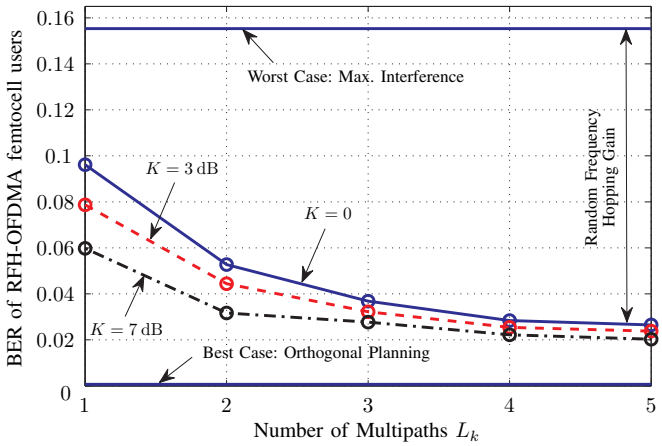

Fig. 10. BER versus number of multipaths and Rice factors (K=0-7dB) in a frequency-selective channel while using uniform random frequency hopping

The performance of random hopping within frequency-selective channels can be seen in Figures 9 and 10. If the line of sight (LOS) between the access point and the user is blocked, we get the results depicted in Fig. 9. A comparison with frequency-nonselective channels (Fig. 8) points out that multipath reception increases the random frequency hopping gain. We get a reduction of the BER introduced by random frequency hopping by more than five times compared to the worst case. As the results of the analytical model in Fig. 9 are derived from the approximation (22), the error compared to simulations is increasing for $L \geq 4$. Finally Fig. 10 shows the impact of the Rice factor in frequency-selective channels. Since the results are a combination of those shown in Figures 8 and 9, the highest random frequency hopping gain can be achieved in a multipath environment with LOS components and it corresponds to a reduction of the BER by a factor of 7.

V. Conclusion

The use of femtocells within existing macrocell infrastructure introduces interference between users of different cells in the downlink as well as in the uplink. Since existing inter-cell interference coordination and self-organization of femtocells is based on knowledge of the cell-environment and on corresponding resource allocation, we introduced random frequency hopping as a self-organization technique. Thus, femtocells are able to integrate themselves into macrocells without exchanging data between the cells or sensing the environment.

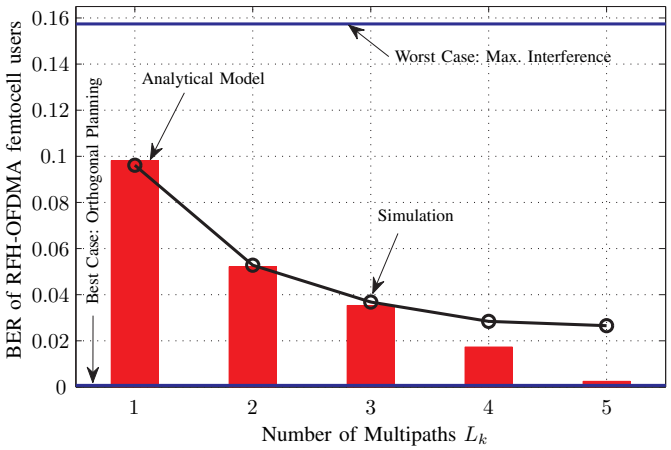

Fig. 9. BER versus number of multipaths in a Rayleigh frequency-selective channel while using uniform random frequency hopping

Therefore random frequency hopping is highly attractive when femtocells have to work immediately after their positioning. We have presented an exact analytical model for the BER when femtocell users employ random frequency hopping and we have applied the model to frequency-nonselective as well as frequency-selective fading. Moreover, all results of the analytical model are verified by simulations. We have shown that random frequency hopping can achieve a reduction of the BER by a factor of 7 compared to systems where the interferer transmits in the same subband as the femtocell user.

Acknowledgment

Part of the work on this paper has been supported by Deutsche Forschungsgemeinschaft (DFG) within the Collaborative Research Center (SFB 876) "Providing Information by Resource-Constrained Analysis", project A4.

References

[1] IDate: *Mobile Traffic Forecasts 2010-2020 and Offloading Solutions*, ICT BeFemto, May 2011
[2] J. Lee, S. Bae, Y. Kwon and M. Chung: *Interference Analysis for Femtocell Deployment in OFDMA Systems Based on Fractional Frequency Reuse*, IEEE Communication Letters, Vol. 15, No. 4, April 2011
[3] I. Guevenc et al: *Interference Avoidance in 3GPP Femtocell Networks Using Resource Partitioning and Sensing*, Symposium on Personal, Indoor and Mobile Radio Communications, Istanbul, Sep. 2010
[4] Z. Bharucha, G. Auer and T. Abe: *Downlink Femto-to-Macro Control Channel Interference for LTE*, Wireless Communications and Networking Conference, Cancun, March 2011
[5] D. Lopez-Perez et al: *Enhanced Intercell Interference Coordination Challenges in Heterogeneous Networks*, IEEE Wireless Communications, Vol. 18, June 2011
[6] S. Rohde et al, *AVIGLE: A System of Systems concept for an Avionic Digital Service Platform Based on Micro Unmanned Aerial Vehicles*, IEEE Systems Man and Cybernetics, Istanbul, 2010
[7] M. Wahlqvist, C. Östberg, J. van de Beek, O. Edfors and P. Brjesson, *A Conceptual Study of OFDM-based Multiple Access Schemes*, Telia Research, Lulea, 1996
[8] Z. Kostic, I. Maric and X. Wang, *Fundamentals of Dynamic Frequency Hopping in Cellular Systems*, IEEE Journal on Selected Areas in Communications, Vol. 19, No. 11, Nov. 2001
[9] B. Jung and D. Sung, *Random FH-OFDMA System Based on Statistical Multiplexing*, Vehicular Technology Conference, Stockholm, June 2005
[10] M. Putzke and C. Wietfeld: *Self-Organizing OFDMA Systems by Random Frequency Hopping*, IFIP Wireless Days, Niagara Falls, Oct. 2011
[11] E. Biglieri, G. Caire, G. Taricco and J. Ventura-Traveset: *Simple Method for Evaluating Error Probabilities*, Electronic letters, Vol. 32, No. 3, 1996
[12] J. Hu and N. Beaulieu: *Accurate Simple Closed-Form Approximations to Rayleigh Sum Distributions and Densities*, IEEE Communications Letters, Vol. 9, No. 2, Feb. 2005
[13] J. Hu and N. Beaulieu: *Accurate Simple Closed-Form Approximations to Ricean Sum Distributions and Densities*, IEEE Communications Letters, Vol. 9, No. 2, Feb. 2005
[14] 3GPP TS 36.211, v. 10.2.0: *Physical Channels and Modulation (Release 10)*, Jun. 2011